EDUCATUM JSMT Vol. 12 Number 2 (2025)
ISSN 2289-7070 / e-ISSN 2462-2451(36-42)
https://ejournal.upsi.edu.my/index.php/EJSMT/index

Hydrometallurgical Synthesis of pure zincite (ZnO) powder from dead zinc carbon batteries for use in the manufacturing of antimicrobial products

Kuranga Ibrahim Ayinla[1,3*], Seyi Ebun Adeboye[3], Mufutau Abiodun Salawu[2], Asim Abdalla. Mohammed[4], Alafara. Abdullahi. Baba[1], Islamiyat. Oluwatosin. Ali[1], Abdulmajeed. Mualiyu[1], Bankim Chandra Tripathy[5]

[1]Department of Industrial Chemistry, University of Ilorin, P.M.B. 1515, Ilorin-240003, Nigeria.
[2]Department of Physics. University of Ilorin, Ilorin, Nigeria
[3]Biotechnology Department, National Biotechnology Development Agency, Abuja, Nigeria
[4]Physics Department, Faculty of Education, University of Zalingei, Sudan
[5]CSIR - Institute of Minerals and Materials Technology, Bhubaneswar-751013, India

**Corresponding author*: ibkuranga@gmail.com, ayinla.ik@unilorin.edu.ng

Received: 29 July 2024; **Accepted:** 1 October 2025; **Published:** 23 October 2025

To cite this article (APA): Ayinla, I. K., Adeboye, S. E., Salawu, M. A., Mohammed, A. A., Baba, A. A., Ali, I. O., Mualiyu, A., & Tripathy, B. C. (2025). Hydrometallurgical Synthesis of pure zincite (ZnO) powder from dead zinc carbon batteries for use in the manufacturing of antimicrobial products. EDUCATUM Journal of Science, Mathematics and Technology, 12(2), 36-42. https://doi.org/10.37134/ejsmt.vol12.2.3.2025

To link to this article: https://doi.org/10.37134/ejsmt.vol12.2.3.2025

Abstract

The conversion of waste materials in our environment into useable chemical products is a popular issue these days. Here, we report on the production of zincite powder using a very simple hydrometallurgical method. Within two hours, 92.23% of the original 10 g/L SZCB reacted at ideal leaching conditions (2.5 mol/L HCl, 80°C). The result predicted the diffusion model as rate determining step, with calculated Ea of 28.53 kJ/mol. The precipitated hydroxide was calcined to produce pure zincite powder of yield 85.2%. Analyses using X-ray diffraction (XRD) and scanning electron microscopy (SEM) revealed that the high purity ZnO existed as a flower-like spherical aggregation and antimicrobial testing was later carried out to be reported in part B of the research.

Keywords: Hydrometallurgy, Kinetics, Metallurgy, Powder Technology, X-ray, Zincite

INTRODUCTION

There are currently a lot of materials that reach the end of their useful lives, and their life cycles are not continuous enough to prevent waste from being created or to permit their reuse as components of other goods [1]. Many of the devices we use today are either gas or battery powered. These two elements have one thing in common: you can utilize them till they run out. When they do, it is customary to either replace the old batteries with new ones or to refill gas. But battery disposal might contribute significantly to environmental waste. In addition, batteries contain a lot of hazardous material and are commonly used. Thus, it might not be a good idea to get rid of them. Recycling your batteries is an alternative to tossing them away [2]. As a result, batteries are regarded as a secondary source of raw material, because important metals such as zinc, manganese, and others can be recovered and sold for use in the production of batteries or other products [3].

Zinc oxides has received a lot of interest recently, owing to its numerous applications and are also among the most promising inorganic compounds with bactericidal activity, and can be found in various biotechnological applications [3-6]. Hence, this study looks into the use of waste zinc-carbon batteries

as a low-cost, unique, and alternative source of zinc oxide (ZnO) to substitute high-priced white zinc compounds (98% purity) in antiseptic manufacture. The production technique was optimized for industrial scaling, and the finished product was analyzed by elemental composition using XRD and EDS, micrograph (SEM), functional group (FTIR), and thermal stability TGA. Further research into the functionality of zincite for antiseptic manufacturing was also suggested.

MATERIALS AND METHODS

Sample collection and preparation

After their use in electronic appliances, spent Zinc-Carbon batteries (SZCBs) of DC 1.5 V size C (R14P) were recovered. The external metal cover, zinc casing, separator, metal caps, carbon rod, and powdered materials were manually separated from the SZCBs. All reagents were of analytical grade (purity greater than 99.9%) and were used without further purification.

Zincite synthesis

Acid leaching and purification experiment

All of the leaching tests were conducted in a 250 mL spherical glass reactor with a mechanical stirrer. For each run, 100 mL of a predetermined molarity HCl solution was added to the reactor and heated to the appropriate temperature using the procedures outlined in [7]. The optimal concentration of hydrochloric acid that resulted in the greatest dissolution (2.5 $mol \cdot L^{-1}$) was then used to optimize other leaching parameters. The solution was purified by precipitating 200 mL of leached liquor with 60 mL of ammonia solution, followed by filtration using a pressure pump machine (HBTJSE1 0.75 kW / 1.0 HP).

Production of zincite (ZnO)

The environmentally benign and inexpensive co-precipitation method was used to produce zincite (ZnO), utilizing 25 mL of 0.5 M NaOH to gradually raise the pH of the pure solution to 9.0 while stirring gently. The resulting precipitate, $Zn(OH)_2$, was filtered, dried in an oven for 8 hours at 90 °C, and calcined at 500 °C in a muffle furnace. The product was finely crushed to obtain a fine powder and subsequently characterized. The rate of ion precipitation was calculated using the appropriate relation.

$$R = [1 - \frac{Co}{Ci}] \times 100 \quad (1)$$

Where R= Precipitation rate and Co and Ci are the concentrations of the specific element in initial and titrated leachate Solution.

Characterization

Elemental analysis was carried out using the X-ray fluorescence (XRF) technique (Philips model 120454/3). Structural characterization was performed using X-ray diffraction (XRD) (PW 3050/60). Scanning electron microscopy (SEM) imaging and energy-dispersive X-ray spectroscopy (EDS) measurements were conducted on a JEOL-700F system, and Fourier-transform infrared (FTIR) analysis of the samples was performed using a Nicolet 6700 analyzer (Thermo Fisher Scientific).

RESULTS AND DISCUSSION

SZCB Leaching optimization and kinetics

The main driving force for zinc dissolving in chloride solution has been observed to be acid concentration [8]. At 55°C, the effect of hydrochloric acid concentration on zinc dissolution was investigated using HCl concentrations ranging from 0.5 to 3 M. The zinc dissolution increased substantially as the HCl concentration increased, as seen in Fig. 1A. The zinc extraction was 24.85% and 75% after 2 hours of leaching at HCl concentrations of 0.5 and 2.5 M, respectively. It is obvious that no additional increase was detected above a concentration of 2.5 M HCl. This could be because metal chloride precipitation is a possibility [9]. Temperature had a considerable impact on the SZCB dissolution process, as Fig. 1B illustrates. After two hours of reaction at 30 °C (47.38%), the zinc extraction was relatively low; nevertheless, it increased with the leaching temperature, reaching a high extraction 92.4% at 65 °C. Thus, it is decided that 65°C is the ideal temperature for SZCB leaching to prevent lose of lixiant due to evaporation [10]. The effect of particle size also investigated and the result is depicted in Fig.1C. As the leaching duration increases and, consequently, the particle diameter decreases the battery dissolution rises. Two hours of leaching for 300 µm and 75 µm particle diameters resulted in 68.02 and 92.43% of the battery ash being dissolved, respectively.

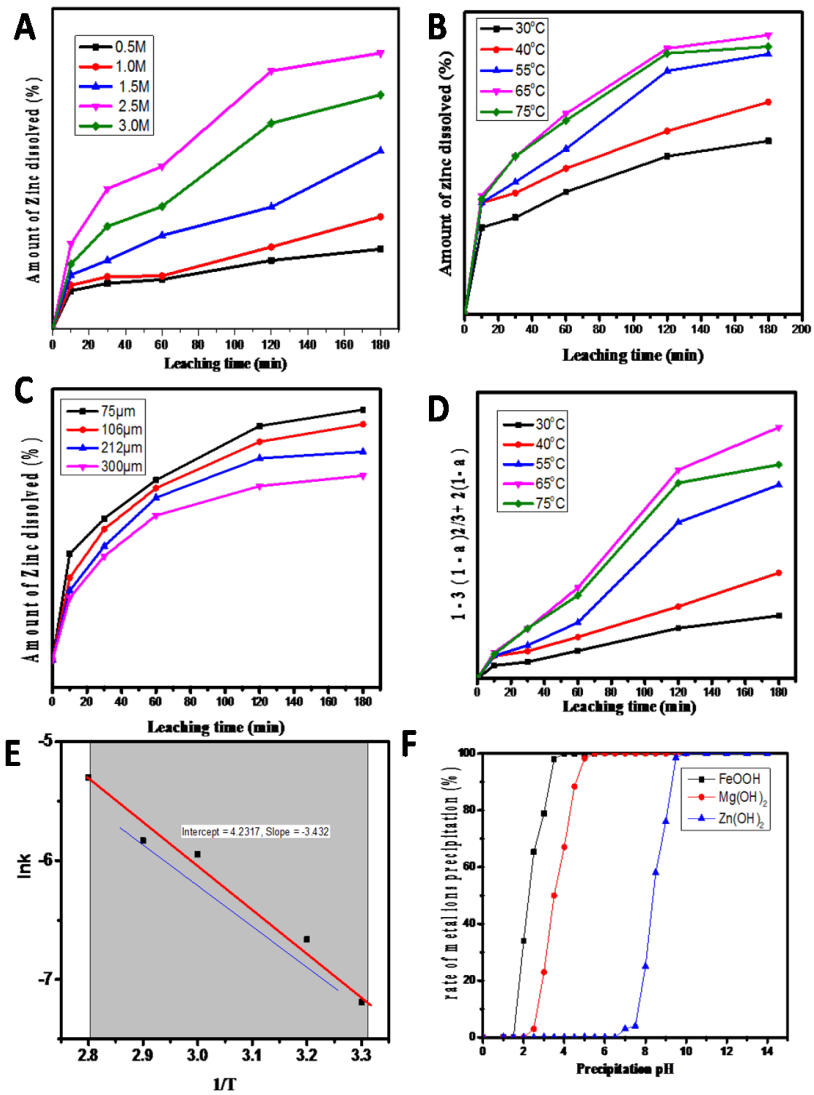

Figure 1. The acid leaching optimization data of SZCB: (A) Acid concentration optimization (B) Temperature optimization (C) Particle diameter(D) shrinking model profile (E) Arrhenius plot (F) Precipitation rate profile

The earlier findings showed the reactivity of SZCB particles during the acid leaching process can be described by the shrinking core model with variable particle size [11] The apparent rate constants fitted

from Fig. 1D were used to create the Arrhenius plot (Fig. 1E) [12]. Activation energy in this case was calculated from the plot to be 28.53 kJ/mol. This indicates that the leaching process's rate-limiting phase obeys liquid film diffusion reaction.

Precipitation rate determination

Figure 1Fshows the simultaneous precipitation efficiency of Fe(III), Zn(II), and Mg(II) at different pH values of ZnCl. The Fe(III) precipitation was higher than 99% at all pH 3.5 conditions but, at pH 4.3, 99% precipitation of Mg(II) was experienced. At pH 9.0, the precipitation efficiency for Zn(II) was 99%, while Mg(II) reached only 2%. The complete precipitation of three metal ions was reached at pH 3.5, 4.0 and 8.5 respectively.

Characterization study

Elemental composition

Using energy dispersive X-ray fluorescence, the chemical makeup of the powder expended battery was ascertained. The powder is mostly made up of tungsten (W = 8.78%), zinc (Zn = 29.44), and manganese (Mn = 18.42) as the major elemental components. Additionally, there was low to trace amounts of lead (Pb = 0.02), silicon (Si = 3.29), aluminum (Al = 1.52), and iron (Fe = 1.24) respectively.

Mineralogical composition

XRD analysis was used to analyze the SZCB, intermediate $Zn(OH)_2$, and ZnO (Fig. 2). The SZCB was found to composed the following minerals: crystalline quartz (SiO2), orthoclase ($Al_2O_3K_2O_6SiO_2$), hematite (Fe_2O_3), muscovite ($KAl_2(Si_3Al)O_{10}(OH,F)_2$), osumilite (K-Na-Ca-Mg-Fe-Al–S), calamine [$Zn_5(CO_3)_2(OH)_6$], and garnet (3(Ca,Fe,Mg)O•(Al,Fe)).

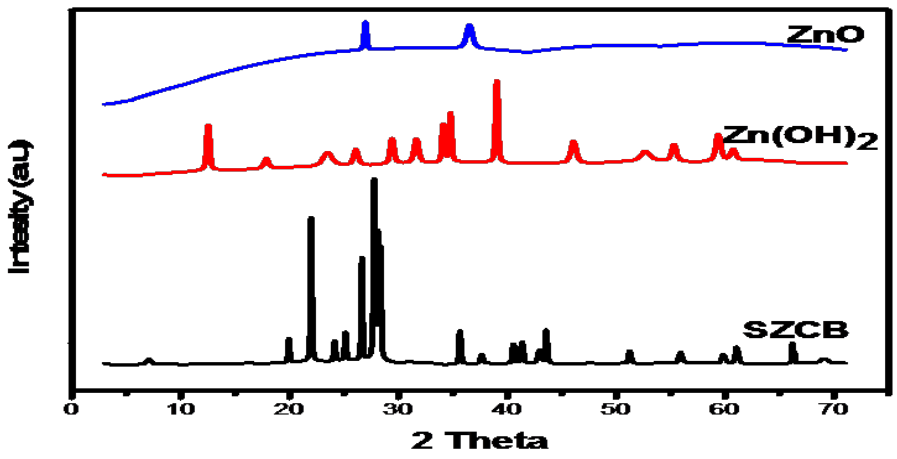

Figure 2. X-ray diffraction pattern of SZCB, intermediate Zn $(OH)_2$, and synthesized ZnO

When comparing the zinc hydroxide (Zn $(OH)_2$) XRD patterns, a little peak shift was seen. Both the raw and intermediate product contain six diffraction peaks at 2θ 30.62, 33.08, 38.0, 45.04, 58.32, and 59.69, which correspond to) diffraction planes of hexagonal $Zn(OH)_2$, respectively. Figure 2 shows most intense peak of ZnO at 2θ = 28.4°, this precisely indexed to orthorhombic $Zn(OH)_2$ (JCPDS: 74-0098) and JCPDS: 78-0225, peaks correspond to hexagonal zincite ZnO. The SEM images of SZCB gave aggregated particles with hexagonal/circular shapes and rough faces (Fig. 3A). A biphasic system formed of irregular particles supporting smaller flocculate-like SiO_2 particles was identified in the case of $Zn(OH)_2$ sample (Fig. 3B). It is important to note in Fig. 3(C), that the entirely flake-like particles in

Fig.3B vanished when the growth temperature was raised to 500°C, leaving only fully trapezoids-like morphology with full agglomeration.

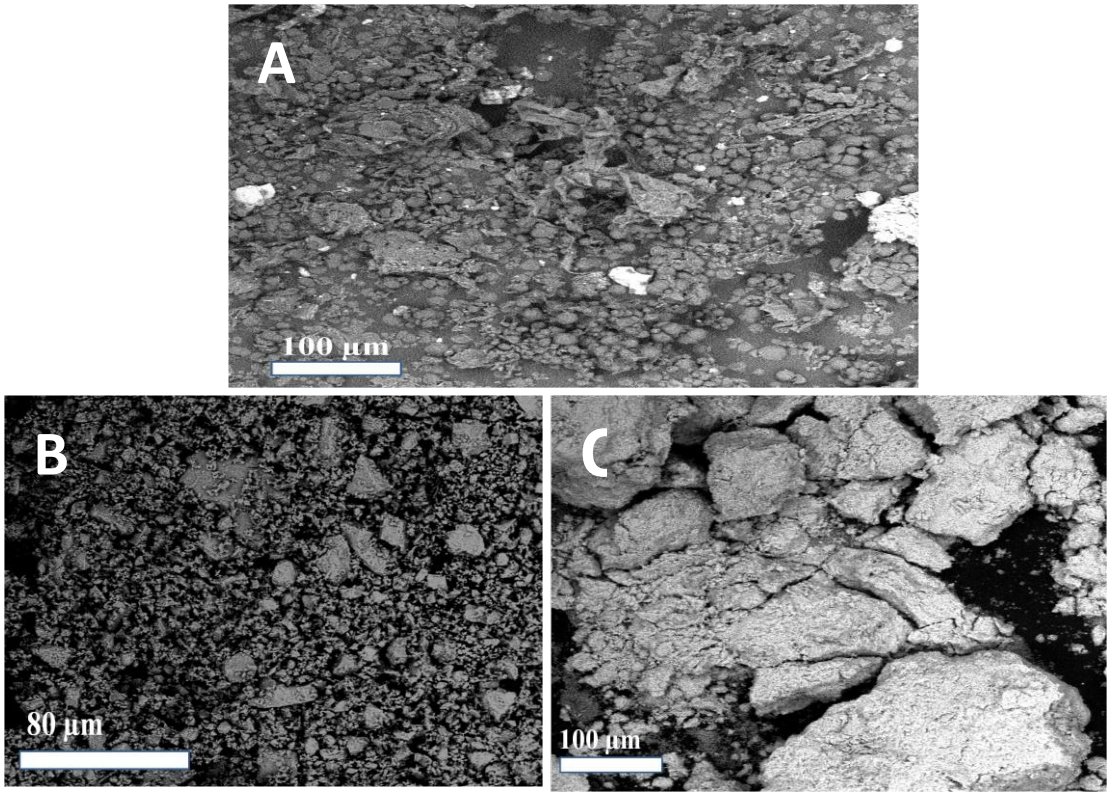

Figure 3. The SEM images of SZCB, $(Zn(OH)_2$ and zincite (ZnO).

Functionality and thermal Characterization of Zincite (ZnO) powder.

The FTIR spectra of ZnO powder sintered at 500°C for 2 hours is shown in Figure 5A. The bands at 545 and 715 cm^{-1} are caused by the stretching mode of Zn-O vibration, and the intensity of this peak was observed to rise with increasing temperature when compared to ZnO powder in the literature [11]. The complete spectrum has showed bands at 3451, 3488, which are related to the broad band expectation of the hydroxyl group of water, and 2070 and 1602 cm^{-1}, which are due to the symmetrical vibration of CH_3 and C=C groups of organic material, which may be traced to hydrocarbon particles encountered in the furnace.

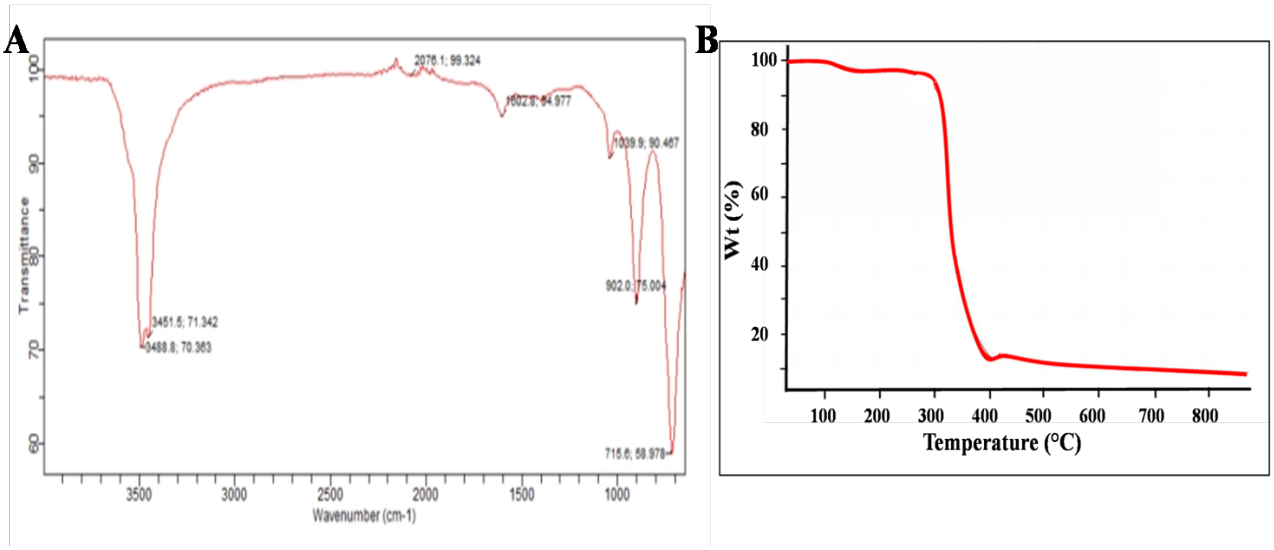

Figure 4. FTIR spectra and TGA profile of synthesized Zincite powder

As expected, Fig. 4B depicts a typical single-step decomposition process in which $Zn(OH)_2$ degraded to create ZnO with the release of H_2O between roughly 180°C and 200°C. However, there is a modest weight change event from 280 °C to 390 °C during this single step, which could be attributed to the presence of two phases and a change in crystal structure.

CONCLUSION

This work successfully established a sustainable and effective hydrometallurgical procedure for producing high-purity zincite (ZnO) powder from used zinc-carbon batteries. The optimized technology produced a ZnO product with a purity of around 98.7%, which was validated by XRD and FTIR characterisation techniques. The actual yield of ZnO powder from the processed battery material was 82.5%, demonstrating an efficient recovery method.. Given the excellent purity and consistent crystallinity of the synthesized ZnO, it is ideal for use in antibacterial applications where purity and structural integrity are crucial to efficacy. Furthermore, the process has tremendous potential for scalability because of its relatively low working temperature, reduced chemical input, and compatibility with continuous processing systems. With proper optimization and waste management integration, the predicted industrial yield might exceed 90%, making this technique both environmentally friendly and economically viable. Thus, the proposed technology provides a feasible pathway for transforming e-waste into value-added antimicrobial materials, thereby promoting circular economy principles in battery waste management.

Acknowledgement

The authors would like to thank the CSIR-Institute of Minerals and Materials Technology in Bhubaneswar for her assistance with sample characterization.

REFERENCES

[1] U. Yogeswaran, U. and Chen, S. M. (2008) A Review on the Electrochemical Sensors and Biosensors Composed of Nanowires as Sensing Material. *Sensors,* 8, 290-313. *http://dx.doi.org/10.3390/s8010290*

[2] Pearton, S. .J., Norton, D. P., Ip, K., Heo, Y.W. & Steiner, T. (2005) Recent Progress in Processing and Properties of ZnO. *Progress in Materials Science*, 50, 293-340.

[3] Kołodziejczak-Radzimska, A., & Jesionowski, T. (2014). Zinc Oxide-From Synthesis to Application: A Review. *Materials (Basel, Switzerland)*, *7*(4), 2833–2881. *https://doi.org/10.3390/ma7042833*

[4] Zanet, V., Vidic, J., Auger, S., Vizzini, P., Lippe, G., Iacumin, L., Comi, G., & Manzano, M. (2019). Activity evaluation of pure and doped zinc oxide nanoparticles against bacterial pathogens and Saccharomyces cerevisiae. *Journal of applied microbiology, 127*(5), 1391–1402. *https://doi.org/10.1111/jam.14407*

[5] Yang, W., Liu, Y., Wang, Q., & Pan, J. (2017). Removal of elemental mercury from flue gas using wheat straw chars modified by Mn-Ce mixed oxides with ultrasonic-assisted impregnation. *Chemical Engineering Journal*, *326*, 169-181.

[6] Dai, Z., Shao, G., Hong, J., Bao, J., & Shen, J. (2009). Immobilization and direct electrochemistry of glucose oxidase on a tetragonal pyramid-shaped porous ZnO nanostructure for a glucose biosensor. *Biosensors and Bioelectronics*, *24*(5), 1286-1291.

[7] Ayinla, I. K. Baba, A. A. Oyinloye, J. S. Olaoluwa, D. T, Ibrahim,A. S. Raji, M. A. Abdulrahman, A. & Ajetomobi, O. O. (2018) Establishment of Dissolution Kinetics and Mechanism of Direct Leaching of Gagi Phosphate Rock in Hydrochloric Acid Solution. *Al-HIK. J. Pure & Applied Sciences,* 6, 37

[8] Ayinla, I. K., Baba, A. A., Babamale, H. F., Padhy, S. K., Adio, O., Ananfi, G. A., ... & Tripathy, B. C. (2019). Hydrometallurgical treatment of biotite ore for production of magnesium hydroxide (Mg (OH) 2) for industrial value addition. *Ife Journal of Science*, *21*(3), 235-244.

[9] Baba, A., Adekola, F., & Owuloye, G. (2010). Leaching of lead from spent motorcycle battery in hydrochloric acid. Part I: dissolution kinetics. *Acta Metallurgica Slovaca*, 16(3), 194-204.

[10] Kim, E., Horckmans, L., Spooren, J., Vrancken, K. C., Quaghebeur, M., & Broos, K. (2017). Selective leaching of Pb, Cu, Ni and Zn from secondary lead smelting residues. *Hydrometallurgy*, *169*, 372-381.

[11] Hoseinzadeh, E., Alikhani, M. Y., Samarghandi, M. R., & Shirzad-Siboni, M. (2014). Antimicrobial potential of synthesized zinc oxide nanoparticles against gram positive and gram negative bacteria. *Desalination and Water Treatment*, *52*(25-27), 4969-4976.

[12] Li, L., Cao, Y., Cui, H., Li, G., Li, Y., Zhang, Y., ... & Chen, B. (2023). Upconversion luminescence thermal enhancement from visible to near infrared and improving temperature sensitivity under high temperature using a second-harmonic generation response. *Materials Today Chemistry*, *29*, 101487.